Supplement of Atmos. Chem. Phys., 17, 13747–13766, 2017
https://doi.org/10.5194/acp-17-13747-2017-supplement

Atmospheric Chemistry and Physics
Open Access

Supplement of

Particulate trimethylamine in the summertime Canadian high Arctic lower troposphere

Franziska Köllner et al.

Correspondence to: Franziska Köllner (f.koellner@mpic.de)

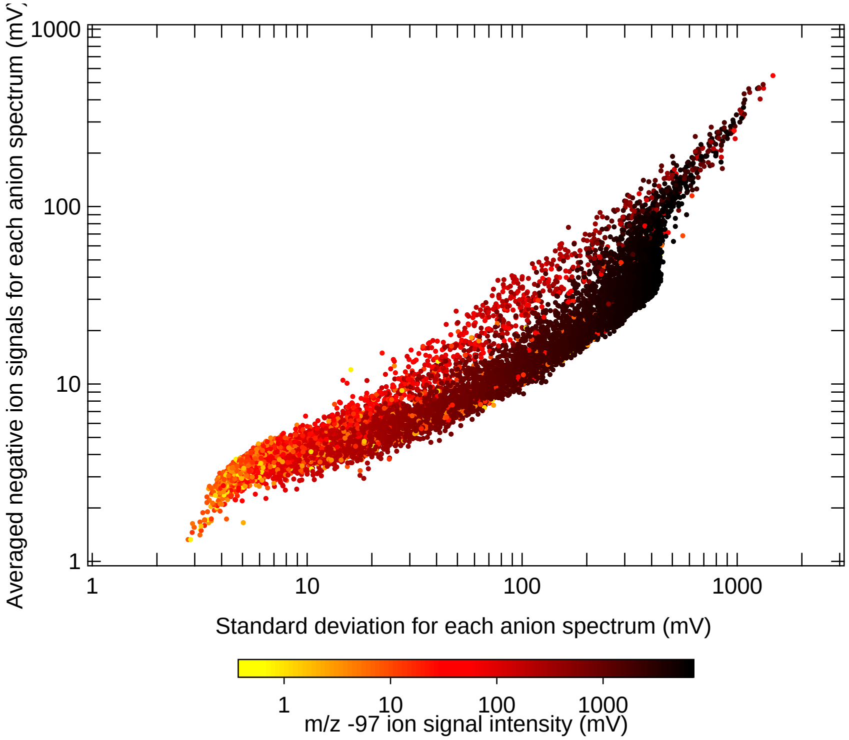

Figure S1. Correlation between average value and standard deviation of the 250 negative ion signal intensities (corresponding to 250 m/z values) of each spectrum. The color-code shows the ion signal intensity at m/z -97 (sulfate).

1 Potential reasons for the lack of negative ions

To describe the lack of anion signals in mass spectra, we calculated for each spectrum an average value and standard deviation of the 250 negative signal intensities (corresponding to 250 m/z values). Small mean values along with small standard deviations indicate mass spectra lack negative ions. Figure S1 demonstrates the distribution of average value and standard deviation of negative ion signals for each spectrum. The colored sulfate ion signals in Fig. S1 further show that the lack of anions corresponds with decreasing sulfate signals. Two main reasons for the lack of negative ions are conceivable. First, negative high-voltages had been temporally switched off. The ALABAMA high-voltages are automatically switched off if the pressure in the mass spectrometer exceeds 5 x 10^{-6} mbar. However, the pressure in the ALABAMA mass spectrometer was always above this critical pressure value during NETCARE 2014. Second, measurements in high relative humidity (RH) environments, in particular marine environments, could explain the lack of anion signals as earlier reported by Neubauer et al. (1998), Spencer et al. (2008) and Guasco et al. (2014). Figure S2 shows the averaged negative ion signal for each spectrum compared to the measured ambient RH and the color-coded ion signal intensity at m/z +39 (potassium). Obviously, averaged negative ion signals at small potassium ion signals (yellow to red colors, Fig. S2) slightly decrease with increasing RH. According to measurements of Neubauer et al. (1998), Spencer et al. (2008) and Guasco et al. (2014), a lack of negative ions in SPMS measurements is likely due to particle water suppression of anion formation. A reason for this observation is not known. However, we further observed anion spectra with enhanced averaged ion signals at high RH, but with the concurrent existence of increased potassium ion signals (red to black colors, Fig. S2). This observation indicates that an internal mixing of particles with potassium may positively affect the intensity of anion signals, although RH is high. Thus far, it is not known if matrix effects may favor the formation of negative ions in the laser ablation and ionization process. To conclude, low potassium ion signals together with high RH environments may negatively affect negative ion formation. This conclusion would further explain the lack of

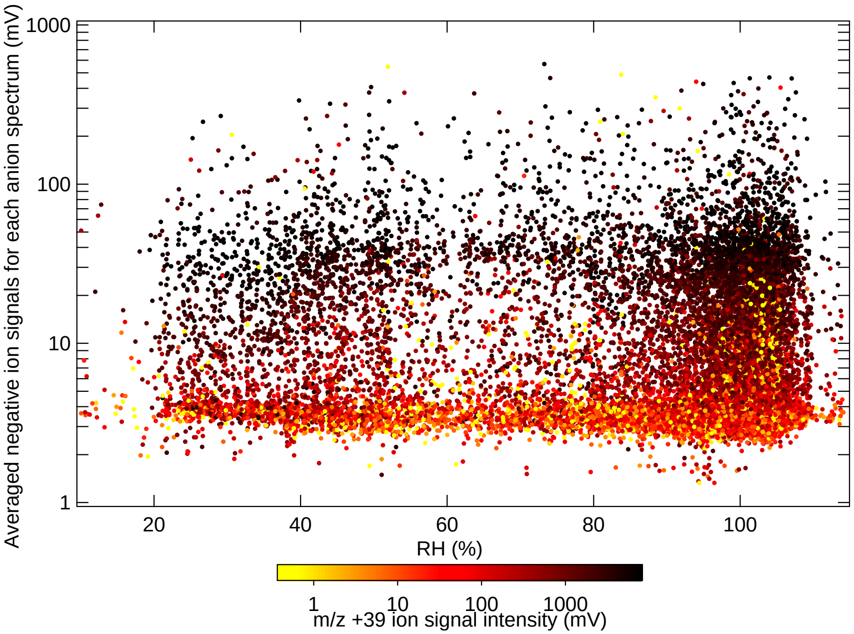

Figure S2. Average value of the 250 negative ion signal intensities (corresponding to 250 m/z values) of each spectrum (see Fig. S1) compared with values of relative humidity (RH). The color-code shows ion signal intensities at m/z +39 (potassium).

negative ions observed in the laboratory mass spectra of TMA-containing particles (even though sulfuric acid was added) (see Supplement Sect. 2).

2 Laboratory measurements of TMA-containing particles

To identify distinct ion markers of TMA in single-particle mass spectra, we conducted laboratory measurements with the ALABAMA. A mixture of TMA dissolved in water, additional milli-q water and sulfuric acid was nebulized with an aerosol generator (PALAS model AGK2000). Afterwards, these droplets passed through a diffusion dryer filled with silica gel to remove water. The particles were size selected with a Differential Mobility Analyzer (TSI model 3080) (set to 300 nm) and then guided into the ALABAMA and an optical particle counter (GRIMM model 1.129).

As can be seen in Fig. S3, the most common mass spectral ion pattern shows peaks at m/z +59 ($(\mathrm{CH_3})_3\mathrm{N}^+$) (molecular ion of TMA) and m/z +58 ($\mathrm{C_3H_8N}^+$). These measurements confirm previous laboratory observations using 266 nm laser desorption/ionization single-particle mass spectrometry (Angelino et al., 2001). Based on the study of Angelino et al. (2001), particulate TMA have been detected in ambient air using SPMS (e.g., Roth et al., 2016; Healy et al., 2015; Rehbein et al., 2011). Further ion signals at m/z +60 and m/z +76 in Fig. S3 could be explained by protonation and oxidation of TMA (Angelino et al., 2001). Despite the addition of sulfuric acid, negative ion mass spectra show poor signals (not shown here). Potential reasons are discussed in the Supplement Sect. 1. The energy of the ablation laser was around 1 mJ/pulse during laboratory measurements. The ablation laser energy deployed during the NETCARE 2014 campaign was between 3 and 4 mJ/pulse. Despite the higher laser ablation energy deployed during NETCARE 2014 compared to lab measurements, the molecular ion of TMA (m/z +59 ($(\mathrm{CH_3})_3\mathrm{N}^+$)) together with ion signals at m/z +58 ($\mathrm{C_3H_8N}^+$) were produced during laser desorption/ionization process.

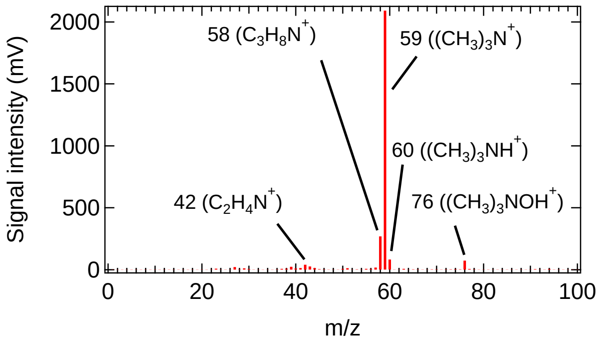

Figure S3. Mean cation spectrum of 88 single particle spectra analyzed within the TMA laboratory measurements.

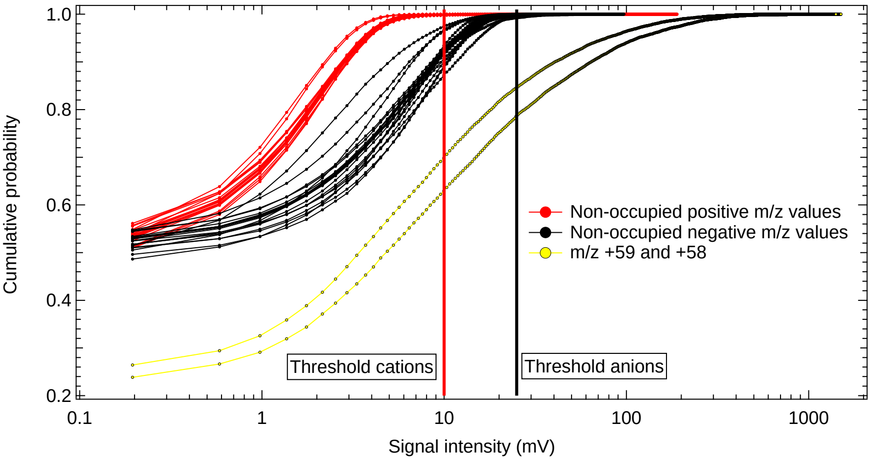

Figure S4. Cumulative probability density functions of signal intensities from different m/z values: m/z +58 and +58 (yellow), m/z -2 to -11 and m/z -245 to -250 (black lines) and m/z +2 to +11 and m/z +245 to +250 (red lines). The vertical red and black lines depict the cation peak area threshold of 10 mV and the anion peak area threshold of 25 mV, respectively.

3 Ion peak area thresholds

The ion peak area threshold describes a certain intensity value in mass spectra that the ion signals have to exceed to be further analyzed. To determine this threshold, we used all ambient single particle mass spectra (in total: 18387) analyzed by the ALABAMA during NETCARE 2014. We further assumed that certain m/z values in single particle mass spectra are likely not occupied by ions produced during laser desorption/ionization, such as m/z (positive and negative) 2-11 and 245-250. Figure S4 presents the cumulative probability of signal intensities belonging to these non-occupied m/z values (black and red lines).
At cumulative probabilities between 99 % and 100 % signal intensities reach 10 mV for positive ions and 25 mV for negative ions (vertical red and black lines). These values are defined as ion peak area thresholds in the analyis.
The cumulative probabilities of the measured ion signals at m/z +59 and +58 (considered as ion markers for TMA in single particle spectra) are further given in Fig. S4. We can use it to estimate the range of uncertainty of the relative fraction of particulate TMA. For example, by shifting the ion peak area threshold - or + 5 mV, 13 % more or 7 % less spectra with signals at m/z +59 would be analyzed.

Table S1. Ion markers and assigned species (with acronyms) used to study the presence of other alkylamines (besides TMA) and amino acid in ambient ALABAMA single particle spectra.

Ion markers	Assigned species (acronyms)	References
m/z +46	Dimethylamine (DMA)	Angelino et al. (2001)
m/z +74	Diethylamine (DEA)	
m/z +86	DEA, Triethylamine (TEA) and/or dipropylamine (DPA)	
m/z +101	TEA	
m/z +102	DPA	
m/z +114	DPA and/or tripropylamine (TPA)	
m/z +143	TPA	
m/z +76	Glycine	Silva and Prather (2000)

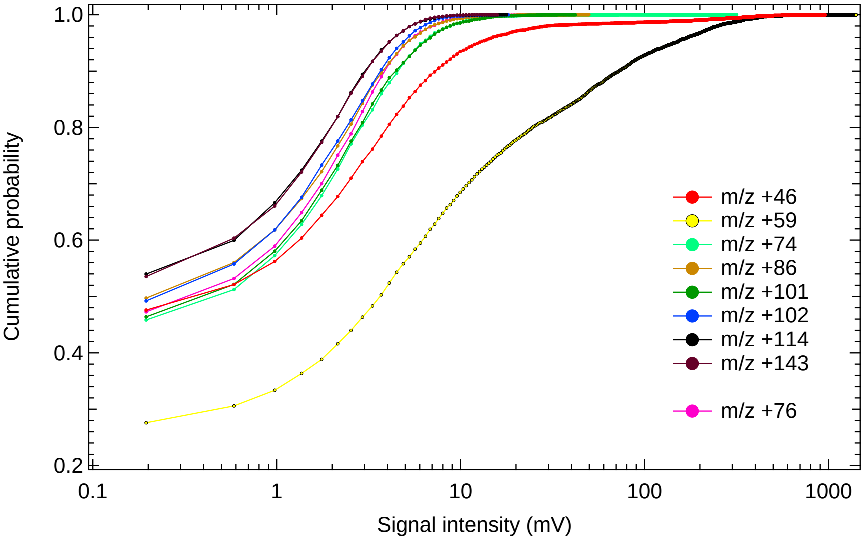

Figure S5. Cumulative probability density functions of signal intensities from different alkylamines and amino acid marker ions (compare to Tab. S1).

4 Identification of other alkylamines and amino acid in single particle mass spectra

Angelino et al. (2001) and Silva and Prather (2000) identified ion markers for several alkylamine and amino acid species using SPMS in the laboratory (Tab. S1). Based on the literature outline above, these substances had been detected in ambient single particle mass spectra as reported in Healy et al. (2015). Healy et al. (2015) further used m/z +46 as ion marker for the identification of dimethylamine (DMA). According to these results, we investigated the occurrence of substances listed in Tab. S1 in ambient single particle mass spectra analyzed by the ALABAMA during NETCARE 2014. Figure S5 demonstrates that none of the ion marker signals for other alkylamines and glycine exceed remarkably the cation ion peak area threshold of 10 mV, except signals at m/z +46. DMA and Na_2^+ show an isobaric interference at m/z +46. To analyze, which of the two compounds produced the ion signals at m/z +46, we compared ion signal intensities at m/z +23 (Na^+) and m/z +46 (DMA and/or Na_2^+) in Fig. S6. It appears that high signal intensities at m/z +46 are accompanied with high signal intensities at m/z +23. Thus, we can infer that ion signals at m/z +46 can be assigned to Na_2^+ rather than DMA^+. Together, none of the alkylamines and amino acid previously identified in SPMS laboratory studies and subsequently detected in ambient aerosol

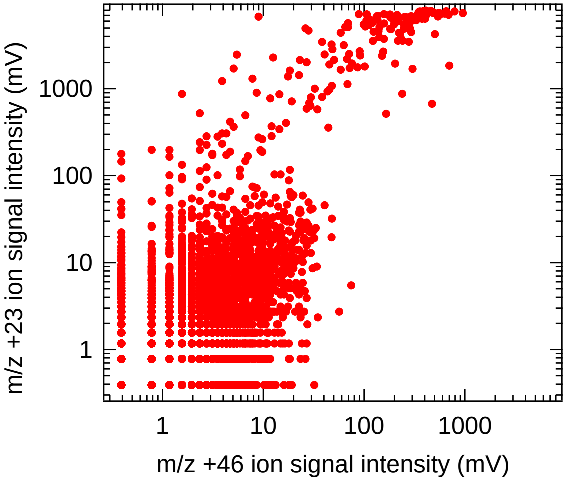

Figure S6. Comparison between m/z +23 and m/z +46 ion signal intensities.

particles can be find in ALABAMA single particle mass spectra sampled in the Arctic during NETCARE 2014 (besides TMA). According to Ge et al. (2011), Gibb et al. (1999), Schade and Crutzen (1995) and Van Neste et al. (1987), it is conceivable that marine-biogenic influenced aerosol particles include different methylamines (such as MA, DMA and TMA). However, the highest emission rates from the ocean were measured for TMA, compared to MA and DMA (e.g., Schade and Crutzen, 1995; Ge et al., 2011). In addition, Van Neste et al. (1987) reported the ocean act as a net sink for DMA. Ge et al. (2011) and Healy et al. (2015) further stated that TMA is the most abundant amine in the atmosphere. Further, previously conducted ALABAMA measurements at mountain Schmücke in Germany showed the occurrence of TMA but no other alkylamines (Roth et al., 2016).

5 Bipolar mean mass spectrum of “others”

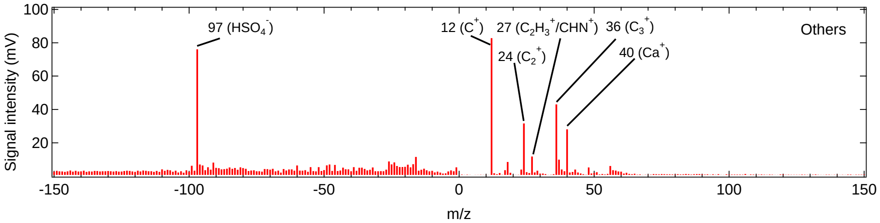

Figure S7. Bipolar mean spectrum of the remaining 736 particles (10 % of mass spectra analyzed by the ALABAMA) that could not be classified into one of the five distinct particle groups. These particles are therefore summarized as “others”.

6 Size- and vertically resolved distribution of TMA-containing particles

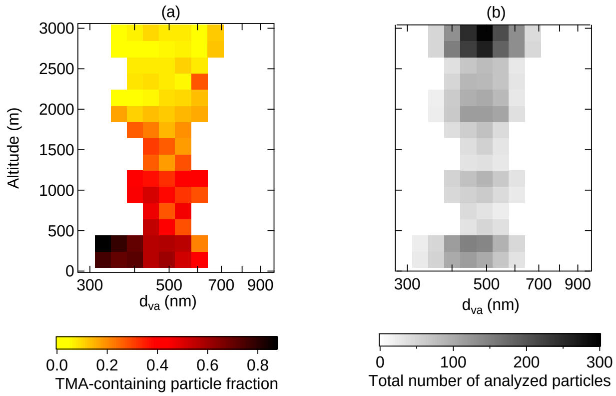

Figure S8. Size- and vertically resolved profiles of: **(a)** TMA-containing particle fraction and **(b)** total number of particles analyzed by the ALABAMA. For statistical reasons, the vertical bin size is 200 m. Grid cells with less than 20 particles in total are not considered.

7 Case study 8 July 2014: Wind speed along the flight track

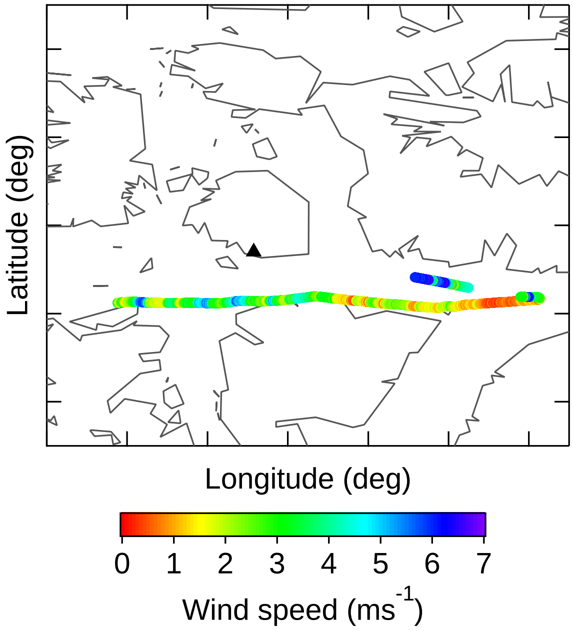

Figure S9. Spatially resolved wind speed (color-coded) below 340 m during the flight on 8 July 2014.

References

Angelino, S., Suess, D. T., and Prather, K. A.: Formation of Aerosol Particles from Reactions of Secondary and Tertiary Alkylamines: Characterization by Aerosol Time-of-Flight Mass Spectrometry, Environmental Science & Technology, 35(15), 3130–3138, doi:10.1021/es0015444, 2001.

Ge, X., Wexler, A. S., and Clegg, S. L.: Atmospheric amines - Part I. A review, Atmospheric Environment, 45, 524 – 546, doi:http://dx.doi.org/10.1016/j.atmosenv.2010.10.012, http://www.sciencedirect.com/science/article/pii/S1352231010008745, 2011.

Gibb, S. W., Mantoura, R. F. C., and Liss, P. S.: Ocean-atmosphere exchange and atmospheric speciation of ammonia and methylamines in the region of the NW Arabian Sea, Global Biogeochemical Cycles, 13, 161–178, doi:10.1029/98GB00743, http://dx.doi.org/10.1029/98GB00743, 1999.

Guasco, T. L., Cuadra-Rodriguez, L. A., Pedler, B. E., Ault, A. P., Collins, D. B., Zhao, D., Kim, M. J., Ruppel, M. J., Wilson, S. C., Pomeroy, R. S., Grassian, V. H., Azam, F., Bertram, T. H., and Prather, K. A.: Transition Metal Associations with Primary Biological Particles in Sea Spray Aerosol Generated in a Wave Channel, Environmental Science & Technology, 48, 1324–1333, doi:10.1021/es403203d, http://dx.doi.org/10.1021/es403203d, pMID: 24328130, 2014.

Healy, R. M., Evans, G. J., Murphy, M., Sierau, B., Arndt, J., McGillicuddy, E., O'Connor, I. P., Sodeau, J. R., and Wenger, J. C.: Single-particle speciation of alkylamines in ambient aerosol at five European sites, Analytical and Bioanalytical Chemistry, 407, 5899–5909, doi:10.1007/s00216-014-8092-1, http://dx.doi.org/10.1007/s00216-014-8092-1, 2015.

Neubauer, K. R., Johnston, M. V., and Wexler, A. S.: Humidity effects on the mass spectra of single aerosol particles, Atmospheric Environment, 32, 2521–2529, 1998.

Rehbein, P. J. G., Jeong, C.-H., McGuire, M. L., Yao, X., Corbin, J. C., and Evans, G. J.: Cloud and Fog Processing Enhanced Gas-to-Particle Partitioning of Trimethylamine, Environmental Science & Technology, 45, 4346–4352, doi:10.1021/es1042113, http://dx.doi.org/10.1021/es1042113, pMID: 21488635, 2011.

Roth, A., Schneider, J., Klimach, T., Mertes, S., van Pinxteren, D., Herrmann, H., and Borrmann, S.: Aerosol properties, source identification, and cloud processing in orographic clouds measured by single particle mass spectrometry on a central European mountain site during HCCT-2010, Atmospheric Chemistry and Physics, 16, 505–524, doi:10.5194/acp-16-505-2016, http://www.atmos-chem-phys.net/16/505/2016/, 2016.

Schade, G. W. and Crutzen, P. J.: Emission of aliphatic amines from animal husbandry and their reactions: Potential source of N2O and HCN, Journal of Atmospheric Chemistry, 22, 319–346, doi:10.1007/BF00696641, https://doi.org/10.1007/BF00696641, 1995.

Silva, P. J. and Prather, K. A.: Interpretation of Mass Spectra from Organic Compounds in Aerosol Time-of-Flight Mass Spectrometry, Analytical Chemistry, 72, 3553–3562, doi:10.1021/ac9910132, http://dx.doi.org/10.1021/ac9910132, pMID: 10952542, 2000.

Spencer, M. T., Holecek, J. C., Corrigan, C. E., Ramanathan, V., and Prather, K. A.: Size-resolved chemical composition of aerosol particles during a monsoonal transition period over the Indian Ocean, Journal of Geophysical Research: Atmospheres, 113, n/a–n/a, doi:10.1029/2007JD008657, http://dx.doi.org/10.1029/2007JD008657, d16305, 2008.

Van Neste, A., Duce, R. A., and Lee, C.: Methylamines in the marine atmosphere, Geophysical Research Letters, 14, 711–714, doi:10.1029/GL014i007p00711, http://dx.doi.org/10.1029/GL014i007p00711, 1987.